

Solution Structure of a Putative HIV1 Immunogenic Peptide: Computer Simulation of the Principal CD4 Binding Domain of gp120

Dan Mihailescu,^{†,‡} Jeremy C. Smith,[†] and Jennifer Reed^{*,‡}

Center for Interdisciplinary Scientific Computation (IWR), Heidelberg University, and Department of Pathochemistry, German Cancer Research Center, D-69120 Heidelberg, Germany

Received June 28, 2001

A 15-residue segment within the principal CD4 binding domain of gp120 from HIV1 is a natural subject for vaccine development. Knowledge of a three-dimensional structure of this peptide in aqueous solution can in principle be used for pharmacophoric footprint identification. However, the peptide is resistant to structural characterization using nuclear magnetic resonance (NMR) due to aggregation properties. Here we examine the conformational properties of the peptide using molecular dynamics simulation. Three simulations were performed starting from widely different structures of the peptide determined by NMR in organic solvents. The three structures converge during the simulations to a common structure in both Cartesian and in backbone dihedral conformational space. Preliminary examination of the average three-dimensional structure identifies, after sequence threading, characteristics of potential use as a pharmacophoric footprint.

Introduction

The extreme sequence variability of the *env* glycoprotein gp120 from HIV 1 has been the primary barrier to the development of an effective vaccine. However, peptide sequence variation can sometimes mask similarities in three-dimensional structure.¹ Earlier work in this laboratory revealed that in many strains a 15-residue segment within the principal CD4-binding domain of gp120 retains the same circular dichroism (CD) spectrum.² This raises the possibility that although there is extreme sequence variation between the strains the segment might still present common structural features that could provide a pharmacophoric “fingerprint”. Additional support for this idea comes from the fact that the various strains of this segment all carry out the same function, that of binding to the CD4 receptor. If identified, and stripped of the incidental masking characteristics present within the wild strains and viral isolates, such a fingerprint might have the capability of eliciting a common immune response that could not then be “escaped” from via multiple mutations. Alternatively, although the segment must adopt a common structure on binding to CD4, it may be insufficiently structured in aqueous solution (the potentially immunogenically interesting state) to permit 3D-fingerprint characterization.

Antigenic epitopes normally comprise not less than five or more than 12 residues, so the 15-residue segment should be sufficient for the purpose of recognition provided that its conformation as a free peptide does not differ significantly from that of the same sequence within the gp120 protein and that it is exposed when gp120 is assembled as a trimer. Evidence that the conformation of the free peptide is similar to that in

gp120 comes from CD and NMR studies on the 15mer which show that when it is embedded in a 44-residue fragment of the native protein its secondary structure is not altered.³ Evidence that the peptide is likely to be exposed when in trimeric form comes from the observation that IgG1 b12, an antibody directed against the CD4-binding domain of gp120,⁴ is effective in neutralizing a wide spectrum of viral strains.

The peptide corresponding to the segment under consideration (residues 400–414 of gp120) has the property of altering its conformation in a cooperative manner from mainly β -hairpin in polar solvent to a 3_{10} helix under polarity conditions similar to those within the cell membrane [e.g., trifluoroethanol (TFE), dimethyl sulfoxide (DMSO)]; this behavior has also been shown to be conserved.² ¹H NMR spectroscopy has been used to obtain detailed structural information on the helical, apolar form.⁵ However, as it is the unbound form in aqueous solution that is of potential interest for immunogenic purposes, it is important to obtain a structural characterization of this form. Unfortunately, the form adopted under polar conditions has an extremely strong tendency to aggregate. At the relatively low protein concentrations required for CD spectroscopy, this aggregation can be avoided, but at the higher concentrations required for ¹H NMR it prevents adequate resolution of the spectra.

During investigations into the mechanism of cooperative folding of this peptide, a series of charged-to-alanine point mutations of the wild-type sequence LPCRIKQFIN-MWQEV was produced, and the effect on folding examined.⁶ It was found that in nonpolar solvent (100% TFE) two of these retain the CD spectrum representative of the β -hairpin form, i.e., that of the wild type in polar solvent. The solution structure of one of the two mutants, R4-A in DMSO, has been solved using ¹H NMR and exhibits a double orthogonal β -hairpin.⁷ This is the same secondary structure content as the native peptide in aqueous solution as determined by CD,

* To whom correspondence should be addressed. Tel: +49-6221-423256. Fax: +49-6221-423259. E-mail: j.reed@dkfz-heidelberg.de.

[†] Heidelberg University.

[‡] German Cancer Research Center.

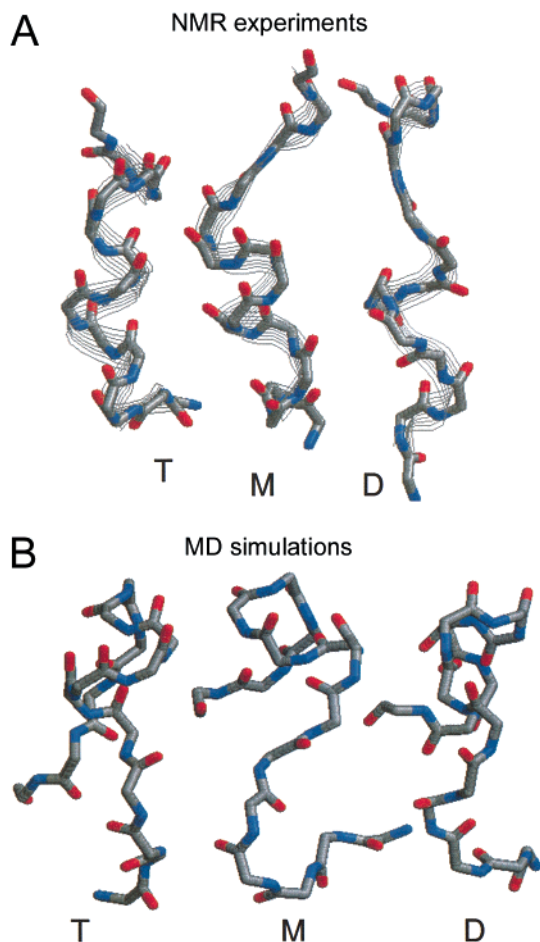


Figure 1. Structures of the LAV 15mer in three organic solvents determined by NMR and after MD simulation in aqueous solution. The structures were superposed to minimize RMS deviations of the backbone atoms and then translated for ease of viewing.

although whether the turns are in the same segments of the peptide sequence is not known.

In the present simulation work, we examine the structure of the wild-type sequence in aqueous solution using molecular dynamics (MD) simulations. Three simulations were performed starting from structures of the peptide determined by NMR in organic solvents: the structure in DMSO (labeled **D**) is a double β -hairpin, that in TFE (labeled **T**) is a 3_{10} helix, and that in a 70:30 methanol/ CCl_4 mixture (labeled **M**) is intermediate between these two forms (see Figure 1). The three NMR structures in organic solvent are representative of different points along the helix to β -strand refolding path observed for the peptide on moving from an apolar to a polar environment, the **T** structure being nearly fully helical, the **M** structure retaining a helix-like fold only in the N-terminal half while the C-terminal half is extended, and the **D** structure having characteristics compatible with the CD spectra of the aqueous form.

The principal question asked here is whether these three dissimilar starting structures, when placed in aqueous solution, converge toward a common structure during the $\sim 10^{-9}$ s time scale accessible to MD. If this turns out to be the case then a starting point for pharmacophoric footprint design may have been obtained. When no convergence is seen it would mean that either the simulations are inaccurate (due to force field

errors or insufficient conformational sampling) or that the peptide is intrinsically too flexible to possess common structural features. The results presented here show that the structures do indeed significantly converge during the simulations. The results are discussed in the context of future possible antigen development.

Methods

The molecular dynamics simulation program used was CHARMM version 27.b2⁸ with the all-atom CHARMM force field version 22.0.⁹ The water model employed was TIP3P¹⁰ modified as in current use in CHARMM. The electrostatic interactions were smoothly brought to zero using the SWITCH method,⁸ which involves multiplication by a cubic function, in this case between 8 and 12 Å. Three simulations were performed of the peptide in aqueous solution. The starting coordinates for these simulations were peptide structures obtained from the NMR experiments in three different solvents: TFE, DMSO, and a 70:30 methanol: CDCl_4 mixture.¹¹

As in the CD and NMR experiments, the sequence of the native peptide was amidated at the C-terminus. The NMR structures determined in DMSO and TFE were of point mutants of the native sequence: glutamine 7 to alanine and arginine 4 to alanine, respectively. For the present calculation these residues were changed back to the native residues by keeping all the unchanged atoms fixed, reconstructing the coordinates for the rest of the atoms from the CHARMM internal coordinates, and still keeping the unchanged atoms fixed, performing a short vacuum energy minimization.

For consistency, all simulations started with the same initial primary box dimensions, $37 \times 37 \times 37 \text{ \AA}^3$. However, due to the differences in the initial peptide structures, the number of water molecules differed slightly in the simulations. The **T** system consisted of one peptide molecule and 1624 water molecules (5145 atoms in total), whereas the **D** and **M** systems consisted of one peptide and 1621 water molecules (5136 atoms in total). The simulations were performed using periodic boundary conditions and in the N (number of molecules) P (pressure) T (temperature) ensemble in which the named parameters are kept constant. Constant pressure algorithms allow the dimensions of the simulated box to vary. These algorithms may be more appropriate for peptide simulation than NV (volume) E (energy) conditions, for which the constant volume can lead to high pressures that might induce spurious conformational behavior. The Langevin piston algorithm was used.¹² This method is suitable for inhomogeneous systems such as aqueous solution biopolymers for two reasons: first, for such systems no large temperature difference between the components of the system is created, and it is thus not necessary to couple the different components to separate heat baths; second, the method has the advantage of not being critically dependent on the choice of piston parameters.

Initially, keeping the peptide fixed, 300 steps of energy minimization using the steepest descent (SD) algorithm were performed followed by 1000 steps with the Newton–Raphson (NR) algorithm. Further energy minimizations with no constraints were performed with 300 steps SD in 5000 steps NR. The minimized system was heated to 300 K, re-scaling the velocities, for 30 ps. The RMS deviations of the backbone atoms from the initial NMR structures at the end of the heating procedure were $< 1 \text{ \AA}$, i.e., only slight alterations from the experimentally determined structures was seen. During the dynamics simulations, the bond lengths involving hydrogen atoms were constrained with the SHAKE algorithm, allowing the use of a 2 fs time step.

During the NPT dynamics simulation, the following parameters were used: the mass of the pressure piston was 100 amu, the Langevin piston collision frequency was 10 ps^{-1} , and the thermal piston mass was 250 kcal ps^2 . An isotropic pressure of 1 atm was applied and the temperature kept constant at 300 K. The NPT productions dynamics were run for 7.5 ns for the **D** and **M** simulations and 17 ns for the **T** simulation.

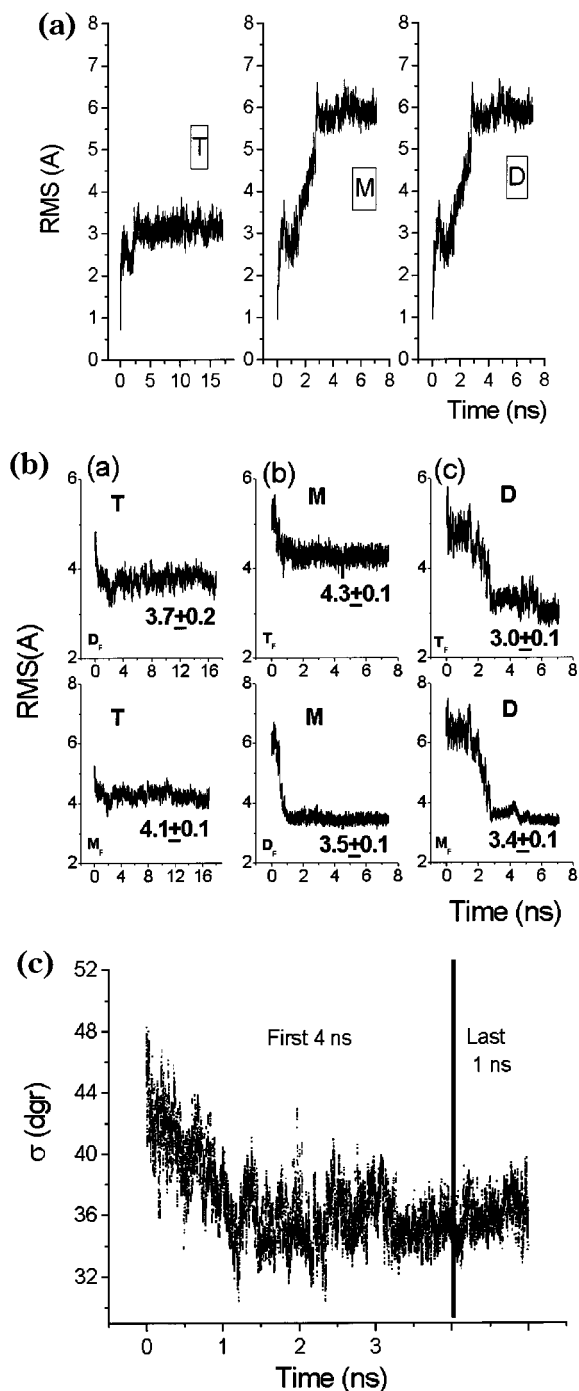


Figure 2. (a, top) Time series of RMS backbone atom deviations of **M**, **T**, and **D** from their starting (NMR) structures. (b, middle) Time series of backbone atom RMS deviations of (a) **M**, (b) **T**, and (c) **D** peptides during the simulation. The deviations from the final structure in the other two simulations, labeled with subscript F, are calculated. Also given are the average and standard deviation RMS values over the last 1 ns of the trajectories. (c, bottom) Time series of the parameter σ (see text for details) for the first 4 ns of the MD trajectories and for the last 1 ns. The vertical bar separates the two time regions.

Results

The backbones of NMR-determined starting structures and the corresponding structures after the MD simulations (averages over the last 1 ns of the trajectories) in water are shown in Figure 1. Figure 2a shows the time series of the RMS coordinate deviation from

the starting structures. In all three simulations most of the deviation takes place in the first 2–4 ns. The RMS deviation values for **D** and **M** at the end of the simulation time are >6 Å. That for **T** is considerably lower, ~ 3 Å.

To examine the convergence properties of the simulations in Cartesian space the RMS deviation was computed between the final frame of any one simulation and each frame of the other two simulations. The results for all possible simulation combinations are shown in Figure 2b. As shown by the $t = 0$ values, initially the structures are 5–6 Å apart from each other. In comparison, the final RMS values are ~ 3 –4 Å. Therefore all pairs of simulations converge toward each other in Cartesian space. Comparison of parts a and b of Figure 2 shows that the time scale of this convergence (~ 1 –4 ns) is similar to that in which the structures deviate from their initial values.

That the structures converge toward each other in Cartesian space does not necessarily imply that they also converge in conformational space. To examine conformational properties, time averages for every Φ and Ψ angle were computed using a running time window of 10 ps. The standard deviation from the mean value of each angle was computed, averaged over the three simulations. This quantity, averaged over the whole sequence, σ , is a measure of the similarity of the three simulations in Ramachandran (backbone torsional) space. Figure 2c shows σ over the first 4 ns and the last 1 ns of the trajectories. Over the first nanosecond, σ reduces significantly, from $\sim 48^\circ$ in the initial ~ 10 ps to $\sim 34^\circ$ and remains fluctuating around this value until the end of the simulation. Therefore, the convergence of the three simulations in Cartesian space is accompanied by a significant shift of the backbone dihedrals toward each other.

Although, as explained earlier, NMR determination of the structure of the entire LAV 15mer in water was not possible, a structure determination in aqueous solution has been made of the N-terminal five residues (plus a sixth that is N-terminal in the native gp120 sequence).¹³ The LPCR tetrad segment of this is required for the conformational transition of the 15mer to 3_{10} helix in nonpolar solution.¹⁴ The backbone dihedrals of the NMR structure for the four residues in common (LPCR) are in good agreement with the simulation values, with an average standard deviation of $\sim 25^\circ$. A Ramachandran plot of the experimental structures and the computed structures (averaged over the final 1 ns) is shown in Figure 3. Figure 3 confirms that the wide spread in the dihedral conformational space of the starting structures is significantly restricted after MD simulation in water. The average standard deviation between the three structures is reduced from $\sim 55^\circ$ for the starting NMR structures to $\sim 34^\circ$. A total of 22 of the 28 angles are in the same conformation in all three simulations (defined here as being within 60° of each other). This compares with only 13 in the starting structures.

Further, the MD structures have shifted toward the extended conformation, a region of Ramachandran space unoccupied in the starting structures.

Secondary structural analysis was performed using the STRIDE software, which computes hydrogen bonds

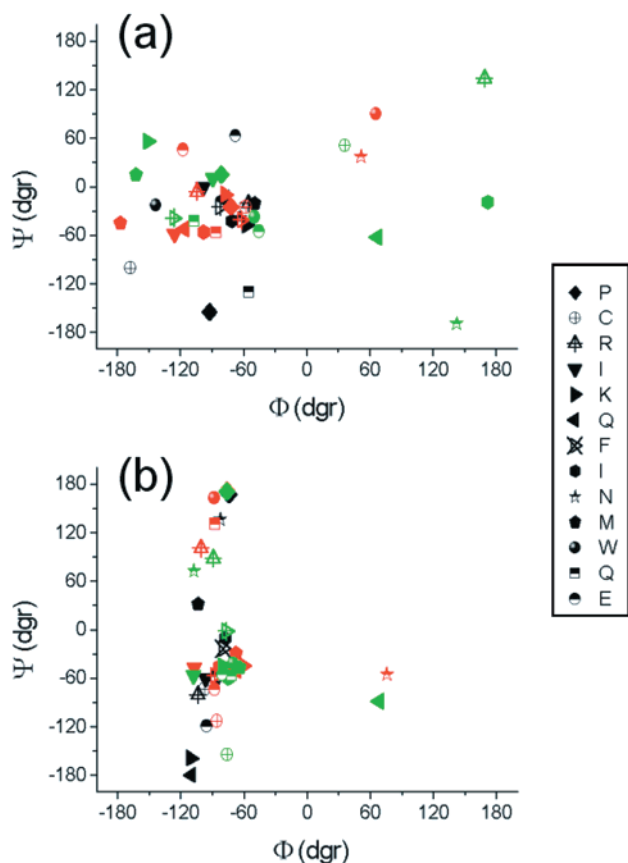


Figure 3. Ramachandran plots of the central 13 residues of the LAV 15mer (first and last amino acid lack defined Φ and Ψ angles): (a) NMR experimental results; (b) time-averaged values for the last 1 ns of the MD trajectories. **T** is shown in black, **M** in red, and **D** in green.

and main chain dihedral angles.¹⁵ The results obtained by applying this algorithm frame-by-frame to the MD

trajectories are shown in Figure 4. In all three simulations the helical regions converted into coil or turn structures. The time required for helix loss varied in the simulations. The initial **M** helix unfolded in ~ 1 ns. In comparison, the helix in the central segment of the **T** starting structure required ~ 9 ns to unfold. Interestingly, the RMS deviation of the **T** backbone from the starting structure did not change dramatically after ~ 3 ns (see Figure 2a). Therefore, modifications of Φ – Ψ angles and H-bond patterns in the 3–9 ns period lead to change in secondary structure in **T** without large displacements in Cartesian space.

Comparing the STRIDE secondary structure assignments at the end of the simulation time, the three structures are quite similar, with coil at the ends of the peptide and turn in the middle. One difference is the persistent coil in the K6Q7 region of simulation **T**. This difference was also observed in corresponding Φ , Ψ dihedral angles (see Figure 2d).

As only a few dihedral angles are in different energy minima in the three final MD structures, segments of the peptides have similar backbone conformations. To quantify this, the coordinates of the backbone, averaged over the last 1 ns of each of the three trajectories, were calculated and the RMS deviations between 4 amino acid segments of the structures computed. The resulting RMS values are presented in Figure 5. The flexibility in the peptide around residues 6–7 can clearly be seen. Two regions can be identified as having particularly high similarities in backbone atom positions (<1.5 Å): residues 1–4 and residues 7–15. After 11 ns of simulation **T**, three segments (1–6, 7–10, and 11–15) of the last 1 ns of the **T**, **M**, and **D** structures were superposable with an RMS of 2–3 Å. Variation between the three simulations was largely due to the dihedrals between residues 6 and 7 and between residues 10 and 11 which acted as hinges. After 17 ns of the **T** simulation, the

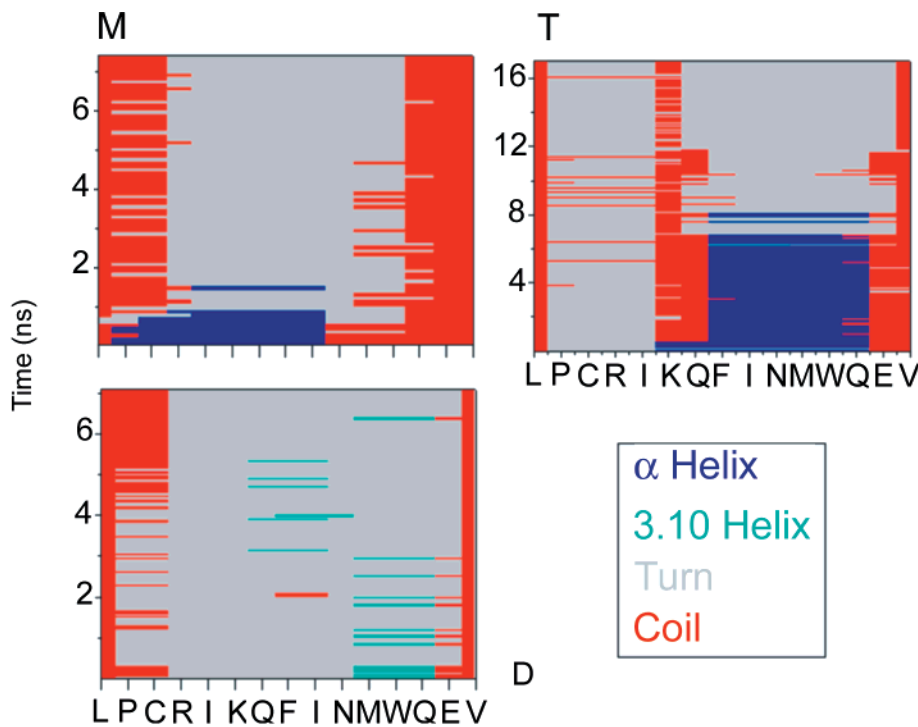


Figure 4. Time series of secondary structure assignments for the three simulations, calculated using STRIDE software.¹⁵

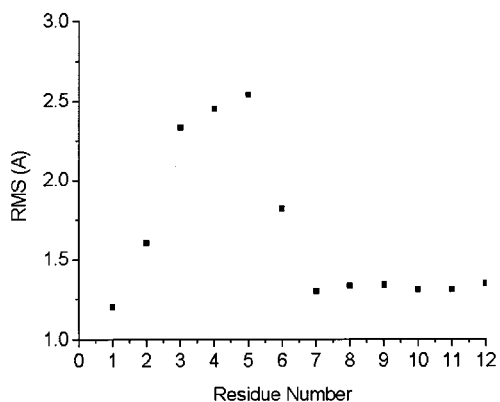


Figure 5. Standard deviation from the mean of backbone atom positions superposed over the last 1 ns of the three simulations. A running average over a four amino acid window was calculated. On the *X* axis, "1" corresponds to the superposition of residues 1–4, "2" to 2–5, ... "12" to 12–15, etc.

structure had converged even closer to **M** and **D**: the dihedral angle variation at residues 10–11 had disappeared, and both the regions 1–6 and 7–15 were superposable to within 2 Å. These superposed structures are shown in Figure 6.

Discussion

The only successful nonpreventative treatment for AIDS to date is highly aggressive antiretroviral therapy (HAART). This generally consists of simultaneous treatment with two reverse transcriptase inhibitors, one acting by substrate competition (NRTI) and one non-nucleosidic inhibitor blocking the active site (NNRTI). These are accompanied by a protease inhibitor or, more rarely, one reverse transcriptase inhibitor is used and two functionally distinct protease inhibitors. The success of HAART lies in just this simultaneous attack at unrelated targets, making it highly unlikely that a single virus will experience simultaneously three sets of serendipitous mutations that would allow it to escape. For this reason drugs targeting yet another entirely different point in viral replication are worth pursuing. However, long-term HAART, although it lowers viremia to undetectable levels, has both financial and metabolic drawbacks.

Recent data indicate that treatment to lower peak viremia during the early, acute phase of infection results in enhanced T-cell production and a lowered set-point for viral load during the chronic phase, often to levels (<11 000 copies) that can then be controlled by the immune system without therapy.^{16,17} It is clear that a high efficiency of intervention in the early phase pays off, and a strong cytotoxic T lymphocyte response to gp120 would be particularly effective in the early phase. But the high variability of the gp120 protein means that antigenic cross reaction between clades is poor. The ideal antigen would be one that exhibited only those characteristics common to all clades. An area of gp120 that would logically be expected to present a conserved pharmacophoric footprint is the domain principally responsible for binding to the CD4 receptor. As our early work had shown that the secondary structure in this domain was conserved,² the obtention of a high-resolution structure of the critical segment may be a useful first step in designing such an ideal antigen.

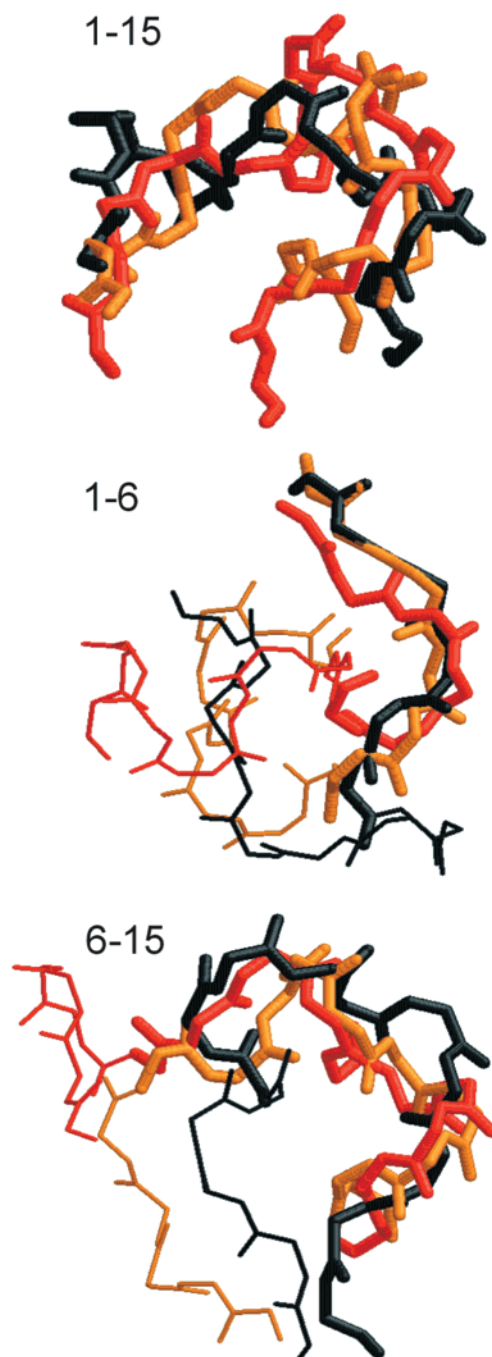


Figure 6. Superposition of the time-averaged backbone structures (last 1 ns of MD trajectories) for all amino acids (1–15), residues 1–6, and residues 6–15. **M** is shown in black, **D** in orange, and **T** in red. Superposed backbone atoms are represented as thick lines and the remaining residues as thin lines.

At the outset of this study, the experimental data available for the LAV 15mer peptide in aqueous solution were limited to (1) CD spectra, which indicated that the peptide had no helical structure under these conditions but existed as a mix of extended chain and turn, and (2) an NMR structure for a hexamer containing the first four N-terminal residues flanked by the two residues N- and C-terminal to these in the sequence in the LAV strain. In addition to these, we had the NMR structure in DMSO of a mutant (R4-A) that CD studies indicate retains the gross secondary structure content of the aqueous form when in organic solvents. A preliminary

MD simulation of the structure of the LAV 15mer in continuum solvent has also been performed.¹⁸ These two latter structures were similar in that both contained two reverse turns oriented at right angles to one another, forming an orthogonal double β -hairpin. However, the position of the second turn differed in that it was shifted two residues toward the N-terminus in the NMR structure relative to its position in the MD structure, a difference that would not be observable with CD.

The aim of the present study was to see whether using advanced simulation techniques in explicit water information could be obtained on the conformational behavior of the peptide in water. In the case that conformational preferences were found, these would be used supplemental to the physical measurements to select a backbone structure to be used in the proposed design of a "universal" HIV antigen. Starting at widely different points in the conformational space of the peptide, defined by NMR structures obtained in different organic solvents, MD simulations were run using explicit water as a solvent. The computations were to be prolonged until either the structures converged to a conformational region with characteristics compatible with the experimental (CD and NMR) data or until it became clear that no convergence would take place. Alternatively, starting structures could have been generated randomly. However, the above approach provides a more rigorous test of convergence. The reason for this is that the physically determined structures are stable entities with established secondary structure that are far removed from one another in both conformational and Cartesian space. As they are intrinsically stable structures energetically, there will be energy barriers to be overcome in converting them into a form stable in aqueous solution. Any convergence seen under these conditions is a strong indication that a single structure is favored in water. In contrast, randomly generated structures tend to be energetically unstable and, with no energy barriers to overcome, convergence would be unnaturally facilitated.

Nanosecond simulations need not, a priori, be long enough for convergence on a peptide of this size. The present simulations almost certainly have not completely converged in the sense that the different accessible states are unlikely to have been visited with probabilities given by the Boltzmann law. However, the results presented here show that in the present case the simulations clearly do converge toward each other sufficiently for the identification of important structural features in common. The three structures converge toward a common region of configurational space, both in Cartesian and in backbone dihedral coordinates. The peptide can be divided into two segments, each of which is within 2 Å after the convergence. Furthermore, the conformation of the N-terminal residues is compatible with that determined using NMR for the N-terminal fragment in water.

From the point of view of medical application, the convergence of the simulations of the LAV 15mer in water gives us a three-dimensional structure that can be used in design of putative lead vaccine. As mentioned in the Introduction, in many strains the peptide conserves the same CD spectrum in aqueous solution. If this corresponds to a conserved three-dimensional structure, then threading the variable sequences onto the

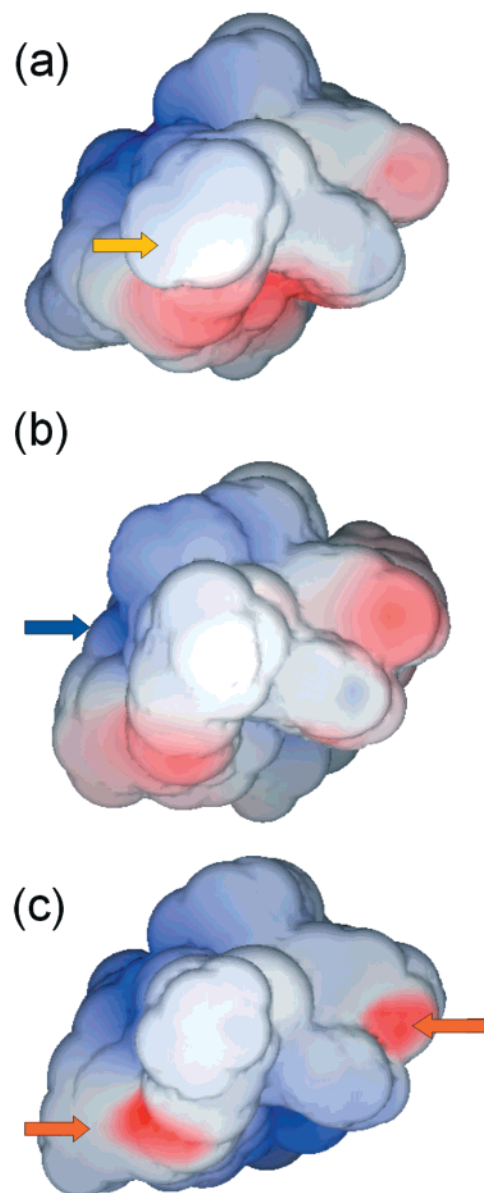


Figure 7. Solvent accessible surfaces (water) for three highly variant strains of HIV1 threaded onto a backbone consisting of the superposable segments 1–6 and 7–15, calculated using an average for the connecting hinge dihedrals (residues 6 and 7). This average structure was slightly adjusted so as to be energetically relaxed by performing a short energy minimization in a box of water. The two other peptide sequences chosen, in addition to the MD-simulated sequence, were LPCRIKQV-VRTWQGV (b) and LPCRIKQIVNLWQRV (c), where the bold residues are changed from the MD-simulated sequence (a). Mutations from the MD-simulated peptide sequence were performed as described in Methods, with the exception that the energy minimization in water was performed keeping the backbone atoms fixed. Negatively and positively charged areas are red and blue, respectively; areas of hydrophobicity are white. Note three conserved features: a positively charged side chain (blue arrow), the central hydrophobic region (yellow arrow), and the negatively charged regions (red arrows) (GRASP software¹⁹).

simulation-derived structure here determined may allow the identification of a common pharmacophoric footprint. Preliminary results, using an "average" dihedral for the residue 6–7 hinge and threading the corresponding 15 residues from three different strains, confirm this possibility (see Figure 7). In the figure one

can see a conserved positive charge (blue arrow), a central hydrophobic cluster, and two areas carrying a negative charge (red arrows). It must be emphasized that this is only an initial estimate of what a pharmacophore might look like. However, the convergence of the majority of the backbone structure to within RMS values that would be acceptable for corresponding crystallographic determinations plus the limited flexibility at the single hinge region means that the structure is likely to be representative of a closely related class of conformers adopted by this epitope. Work is now in progress to establish which of these features persist among different clades, to characterize the entire set of conserved physicochemical properties, and to use these to design an antigen with the aim of provoking a strain-independent immune response. More generally, the present work demonstrates the usefulness of the MD computer simulation method in providing information on the structure of peptides that are resistant to determination by experimental methods.

References

- (1) Murzin, A. G.; Brenner, S. E.; Hubbard, T.; Chothia, C. SCOP: a structural classification of proteins database for the investigation of sequences and structures. *J. Mol. Biol.* **1995**, *247*, 536–540.
- (2) Reed, J.; Kinzel, V. A conformational switch is associated with receptor affinity in peptides derived from the CD4-binding domain of gp120 from HIV I. *Biochemistry* **1991**, *30*, 4521–4528.
- (3) Reed, J.; Kinzel, V. Unpublished results.
- (4) Burton, D. R.; Barbas, C. F., 3rd; Persson, M. A.; Koenig, S.; Chanock, R. M. et al. A large array of human monoclonal antibodies to type 1 human immunodeficiency virus from combinatorial libraries of asymptomatic seropositive individuals. *Proc. Natl. Acad. Sci. U.S.A.* **1991**, *88*, 10134–10137.
- (5) Graf von Stosch, A.; Jimenez, M. A.; Kinzel, V.; Reed, J. Solvent polarity-dependent structural refolding: a CD and NMR study of a 15 residue peptide. *Proteins* **1995**, *23*, 196–203.
- (6) Graf von Stosch, A.; Kinzel, V.; Pipkorn, R.; Reed, J. Investigation of the structural components governing the polarity-dependent refolding of a CD4-binding peptide from gp120. *J. Mol. Biol.* **1995**, *250*, 507–513.
- (7) Faber, M.; Reed, J.; Kinzel, V. Unpublished results (coordinates available from J.R. on request).
- (8) Brooks, B. R.; Brucoleri, R. E.; Olafson, B. D.; States, D. J.; Swaminathan, S.; Karplus, M. CHARMM: A program for macromolecular energy, minimization and dynamics calculations. *J. Comput. Chem.* **1983**, *4*, 187–217.
- (9) MacKerell, J. A. D.; Bashford, D.; Bellott, M.; Dunbrack, R. L., Jr.; Evensen, J. D.; Field, M. J.; Fischer, S.; Gao, J.; Guo, H.; Ha, S.; Joseph-McCarthy, D.; Kuchnir, L.; Kuczera, K.; Lau, F. T. K.; Mattos, C.; Michnick, S.; Ngo, T.; Nguyen, D. T.; Prodhom, B.; Reiher, I. W. E.; Roux, B.; Schlenkrich, M.; Smith, J. C.; Stote, R.; Straub, J.; Watanabe, M.; Wiorkiewicz-Kuczera, J.; Yin, D.; Karplus, M. All-atom empirical potential for molecular modeling and dynamics studies of proteins. *J. Phys. Chem. B* **1998**, *102*, 3586–3616.
- (10) Jorgensen, W. L.; Chandrasekhar, J.; Madura, J. D.; Impey, R. N.; Klein, M. L. Comparison of simple potential functions for simulating liquid water. *J. Chem. Phys.* **1983**, *79*, 926–935.
- (11) Lindemann, A.; Kinzel, V.; Reed, J. Unpublished results (coordinates available from J. R. on request).
- (12) Feller, S. E.; Zhang, Y.; Pastor, R. W.; Brooks, B. R. Constant pressure molecular dynamic simulation: The Langevin piston method. *J. Chem. Phys.* **1995**, *103*, 4613–4621.
- (13) Lindemann, A.; Kinzel, V.; Rosch, P.; Reed, J. Structure of the LAV6 peptide: a nucleation site for the correct receptor-induced refolding of the CD4-binding domain of HIV1 gp 120. *Proteins* **1997**, *29*, 203–211.
- (14) Reed, J.; Kinzel, V. Primary structure elements responsible for the conformational switch in the envelope glycoprotein gp120 from human immunodeficiency virus type 1: LPCR is a motif governing folding. *Proc. Natl. Acad. Sci. U.S.A.* **1993**, *90*, 6761–6765.
- (15) Frishman, D.; Argos, P. Knowledge-based protein secondary structure assignment. *Proteins* **1995**, *23*, 566–579.
- (16) Barouch, D. H.; Santra, S.; Schmitz, J. E.; Kuroda, M. J.; Fu, T.-M.; Wagner, W.; Bilska, M.; Craiu, A.; Zheng, X. X.; Krivulka, G. R.; Beaudry, K.; Lifton, M. A.; Nickerson, C. E.; Trigona, W. L.; Punt, K.; Freed, D. C.; Guan, L.; Dubey, S.; Casimiro, D.; Simon, A.; Davies, M. E.; Chastain, M.; Strom, T. B.; Gelman, R. S.; Montefiori, D. C.; Lewis, M. G.; Emini, E. A.; Shiver, J. W.; Letvin, N. Control of viremia and prevention of clinical AIDS in rhesus monkeys by cytokine-augmented DNA vaccination. Keystone Symposium “AIDS Vaccines in the New Millennium”; Keystone, CO, 2001.
- (17) Altfeld, M.; Rosenberg, E. S.; Shankarappa, R.; Mukherjee, J. S.; Hecht, F.; Eldridge, R. L.; Addo, M. M.; Poon, S. H.; Phillips, M. N.; Robbins, G. K.; Sax, P. E.; Boswell, S.; Kahn, J. O.; Brander, C.; Goulder, P. J.; Levy, J. A.; Mullins, J. I.; Walker, B. D. Abstract Immune control of HIV infection. Keystone Symposium “AIDS Vaccines in the New Millennium”; Keystone, CO, 2001.
- (18) Graf von Stosch, A.; von der Lieth, C. W.; Reed, J. Molecular dynamics study of the proposed beta-hairpin form of the switch domain from HIV1 gp120 alone and complexed with an inhibitor of CD4 binding. *Proteins* **1999**, *34*, 197–205.
- (19) Nicholls, A.; Sharp, K. A.; Honig, B. Protein folding and association: insights from the interfacial and thermodynamic properties of hydrocarbons. *Proteins* **1991**, *11*, 281–296.

JM0109715